Positive Matrix Distribution Schemes for Hyperbolic Systems, with application to the Euler Equations

Edwin van der Weide and *Herman Deconinck* [1]

Abstract. Monotone shock capturing matrix distribution schemes on unstructured grids for solving hyperbolic systems with non-commuting Jacobians are presented. The standard first order upwind scheme on unstructured grids is reviewed and a compact stencil second order version is presented. The optimal first order system scheme is introduced, generalizing a previously developed multidimensional upwind scheme for scalar convection, and a compact second order extension is discussed. For steady state computations, additional benefits are demonstrated by applying the system schemes to an optimally decoupled pseudo-unsteady form of the equations obtained by using preconditioning. Numerical validation on transonic flows confirm the potential of the compact stencil schemes.

1 INTRODUCTION

The development of multidimensional upwind methods for solving *scalar convection* equations has led to improved schemes on compact stencils, compared to the standard finite volume schemes based on MUSCL reconstruction [3], [7] . As these multidimensional scalar schemes do not rely on dimensional splitting, their application to non-commuting systems is not trivial.

The most successful extension for solving the steady state Euler equations until now is based on a splitting of the system in its hyperbolic and elliptic contributions, which are then treated by different schemes. Such a splitting is derived by using local preconditioning : A pseudo-unsteady form of the equations is obtained with 2 uncoupled scalar convection equations for entropy and total enthalpy (both in 2D and 3D), and a coupled system for 2 acoustic variables in 2D [12]. In 2D supersonic flow, the acoustic subsystem further decouples in two scalar convection equations along the Mach lines and the ideal situation of 4 scalar convection equations is reached. In 2D subsonic flow the acoustic system remains coupled and application of scalar convection schemes is at least questionable. In 3D there is 1 additional coupled shear equation and the acoustic equations remain coupled even in supersonic flow.

[1] von Karman Institute for Fluid Dynamics, Waterloose Steenweg 72, Sint-Genesius-Rode, Belgium

ECCOMAS 96.
Published in 1996 by John Wiley & Sons, Ltd.

In the past two approaches have been followed for the treatment of the acoustic subsystem:

1: Treat the coupling terms as source terms and distribute them with a non-positive scalar distribution scheme [9]. The consequence is that the discretization is no longer guaranteed monotonic, and robustness problems have been encountered for normal shocks, especially in 3D.

2: Use a system Lax-Wendroff [5] or system SUPG finite element distribution [8]. Both need an additional shock capturing dissipation to handle the subsonic part of strong shocks since the basic schemes are not monotonic.

In 3D the situation is even worse since even the supersonic acoustic part of the flow cannot be handled by the scalar convection schemes.

In the present paper a completely different approach is followed, based on positive matrix distribution schemes which are a generalization of the scalar convection schemes to systems. These system schemes are constructed such that for any decoupled equation in the system they automatically reduce to the scalar distribution scheme on which they are based. In fact, if the starting scheme is first order upwinding, the matrix scheme becomes a close variant of the standard Roe-scheme, only differing in the linearization. The optimal first order system scheme is much less diffusive while remaining guaranteed monotonic and generally applicable through the sonic point. Second order extensions are discussed, which are totally different from the standard schemes by the compactness of their stencil.

As the schemes are general, they can be applied to the original Euler system. When they are applied to the optimally decoupled preconditioned equations, additional benefits are obtained, e.g. total enthalpy is preserved up to machine zero even in the intermediate shock points.

2 RESIDUAL DISTRIBUTION SCHEMES

Consider the unsteady hyperbolic system of equations in two space dimensions given by

$$\frac{\partial \mathrm{W}}{\partial \mathrm{t}} + \mathrm{A_W}\frac{\partial \mathrm{W}}{\partial \mathrm{x}} + \mathrm{B_W}\frac{\partial \mathrm{W}}{\partial \mathrm{y}} = 0. \tag{1}$$

Assume further that this system has been linearized over a triangular computational cell Ω (see below), such that the Jacobian matrices $\mathrm{A_W}$ and $\mathrm{B_W}$ are constant. Using Gauss' theorem the residual in integral form of equation (1) over cell Ω is

$$\phi^{\Omega} = \iint_{\Omega} \left(\mathrm{A_W} \frac{\partial \mathrm{W}}{\partial \mathrm{x}} + \mathrm{B_W} \frac{\partial \mathrm{W}}{\partial \mathrm{y}} \right) \mathrm{d}\Omega \tag{2}$$

$$= \oint_{\Gamma} \mathrm{W} \left(\mathrm{A_W} \mathrm{n}_{\mathrm{x_{ext}}} + \mathrm{B_W} \mathrm{n}_{\mathrm{y_{ext}}} \right) \mathrm{d}\Gamma, \tag{3}$$

where ϕ^{Ω} is the vector containing the cell residuals, Γ is the boundary of the control volume Ω and $\mathrm{n}_{\mathrm{x_{ext}}}$ and $\mathrm{n}_{\mathrm{y_{ext}}}$ are respectively the x and y component of the outward normal. In the residual distribution approach, the contour integral is evaluated using the unknowns stored at the corners, and fractions of ϕ^{Ω} are sent to the cell vertices. Assembling the contributions from all cells the nodal update is obtained. The semi-discretization in point i is then

$$\frac{\mathrm{dW_i}}{\mathrm{dt}} = -\frac{1}{\mathrm{S_i}} \sum_{\Omega} \beta_{\mathrm{i}}^{\Omega} \phi^{\Omega}. \tag{4}$$

Here $\mathrm{S_i}$ is the area of the median dual cell around node i, see figure 1, and $\beta_{\mathrm{i}}^{\Omega}$ is the distribution matrix to node i. For consistency one has $\sum_{\mathrm{j}} \beta_{\mathrm{j}}^{\Omega} = \mathrm{I}$, where the summation extends over all vertices of a cell. The properties of the different

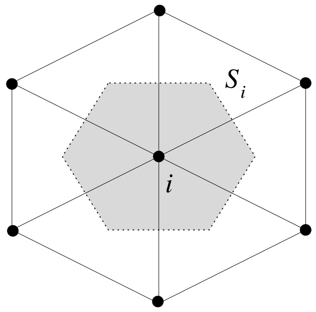

Figure 1. Area of the median dual cell $\mathrm{S_i}$ of node i

schemes are determined by the way $\beta_{\mathrm{i}}^{\Omega}$ is defined. Important properties are:

- **Positivity**
  A monotonic scheme can be obtained by demanding positivity. Suppose that the numerical solution at mesh point i is $\mathrm{W_i}$. Then the positivity property requires that in the semi-discrete form of equation (1),

$$\frac{\mathrm{dW_i}}{\mathrm{dt}} \mathrm{S_i} = -\sum_{\mathrm{k} \neq \mathrm{i}} \mathrm{C_{ki}} (\mathrm{W_i} - \mathrm{W_k}), \tag{5}$$

  the matrices $\mathrm{C_{ki}}$ are all positive semi-definite, which is a generalization of the scalar positivity also called Local Extremum Diminishing (LED) property. Condition (5) is called global positivity and is difficult to impose. Therefore a more restricted property, local positivity see [3], is introduced. This means that condition (5) is imposed for the contribution of every cell, which is very easy to check.
- **Linearity Preservation or Residual Property**
  Second order truncation error in the steady state is obtained by demanding that no updates are sent to the vertices if the cell residual is zero. This property is also known as k-exactness for linear polynomials. This is satisfied when the distribution matrices $\beta_{\mathrm{i}}^{\Omega}$ are bounded, such that

$$\beta_{\mathrm{i}}^{\Omega} \phi^{\Omega} \to 0 \qquad \textit{when} \qquad \Phi^{\Omega} \to 0. \tag{6}$$

  It can be proven that only non-linear schemes can satisfy positivity and linearity preservation at the same time (Godunov's theorem).
- **Conservative linearization**
  The matrix distribution schemes are based on the quasi-linear form of the equations. For solutions with discontinuities the conservative form must be solved to obtain the correct jump relations. The link between the two formulations is given by the conservative linearization briefly discussed here [2]. The quasi-linear form of the equations is conservative if for any cell Ω the relation

$$\oint_{\Gamma} \vec{\mathrm{F}} \cdot \vec{\mathrm{n}} \, \mathrm{d}\Gamma \equiv \frac{\partial \vec{\mathrm{F}}}{\partial \mathrm{V}} \left(\bar{\mathrm{V}} \right) \cdot \oint_{\Gamma} \mathrm{V} \, \vec{\mathrm{n}} \, \mathrm{d}\Gamma \tag{7}$$

  is identically satisfied. Here V is an arbitrary set of independent variables, $\bar{\mathrm{V}}$ a cell-averaged state of the variables V, $\vec{\mathrm{F}}$ the conservative flux vector and Γ the edge of the cell. A good choice for the variables V on *triangular* cells is the Roe parameter vector Z, defined in two space dimensions by $\mathrm{Z} = (\sqrt{\rho}, \sqrt{\rho}\mathrm{u}, \sqrt{\rho}\mathrm{v}, \sqrt{\rho}\mathrm{H})^{\mathrm{T}}$. Indeed, it has been shown that simple arythmetic averaging of Z over the vertex values satisfies (7), thus extending 1D Roe-averaging in two and three space dimensions (using tetrahedra in 3D).

3 FIRST ORDER MATRIX DISTRIBUTION SCHEMES

An essential parameter for the distribution schemes is the jacobian matrix K, defined as

$$\mathrm{K} = \left(\mathrm{A_W} \mathrm{n_x} + \mathrm{B_W} \mathrm{n_y} \right), \tag{8}$$

where $\mathrm{n_x}$ and $\mathrm{n_y}$ are the x and y component of a scaled normal. K can be written as

$$\mathrm{K} = \mathrm{R} \Lambda \mathrm{L}, \tag{9}$$

where the columns of R contain the right eigenvectors, Λ is a diagonal matrix of the eigenvalues and $\mathrm{L} = \mathrm{R}^{-1}$. As the system (1) is hyperbolic, the matrices R, Λ and L will be real. The matrices K^{+} and K^{-} are given by

$$\mathrm{K}^{+} = \mathrm{R} \Lambda^{+} \mathrm{L}, \qquad \mathrm{K}^{-} = \mathrm{R} \Lambda^{-} \mathrm{L}. \tag{10}$$

Here Λ^{+} contains the positive and Λ^{-} the negative eigenvalues, $\Lambda^{\pm} = \frac{\Lambda \pm |\Lambda|}{2}$.

3.1 The system first order FV-scheme

We discuss first the residual distribution variant of the first order finite volume (FV) scheme on the median dual mesh with normals $\vec{n}_{12}$, $\vec{n}_{23}$ and $\vec{n}_{31}$, see figure 2. As the solution

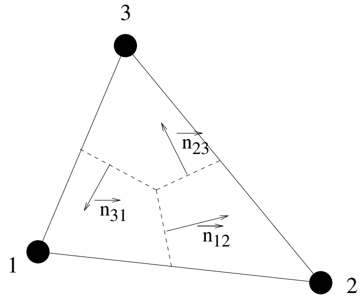

Figure 2. Normals for the FV-scheme

is stored in the vertices of the triangle the contour integral in equation (3) is calculated numerically with the trapezium rule, giving in terms of the dual grid normals

$$\phi^{\Omega} = K_{12}(W_2 - W_1) + K_{23}(W_3 - W_2) + K_{31}(W_1 - W_3), \tag{11}$$

where the matrices K_{ij} are defined following eqn (8) in combination with the normals $\vec{n}_{ij}$. The first order finite volume scheme is then obtained by distributing the different terms of ϕ^{Ω} to the vertices of the cell according to the sign of the eigenvalues of the matrices K_{ij},

$$\phi_i^{FV} = \beta_i^{FV}\phi^{\Omega} = K_{ij}^{+}(W_i - W_j) + K_{ki}^{-}(W_k - W_i), \tag{12}$$

where (i,j,k) is any circular permutation of $(1,2,3)$. Combining equations (4), (5) and (12) shows that this scheme is indeed positive and only first order (the $\beta_i^{FV}\phi^{\Omega}$ do not tend to zero for vanishing residual ϕ^{Ω}). It differs from the standard Roe scheme only in the way the linearization is defined, which is cell-wise in the present variant as discussed before.

3.2 The system first order N-scheme

The scheme described in the previous paragraph is indeed very robust and relative simple, but it is not the most accurate positive first order scheme. For the *scalar convection* case this optimal first order scheme (called N-scheme) has been proposed by Roe, see e.g. [3]. Briefly summarizing the scheme for the scalar convection equation $w_t + \vec{\lambda}\vec{\nabla} w = 0$, the residual is distributed to the downstream vertices in the following way:
1: If the triangle has only one inflow side, the entire residual is sent to the unique downstream node opposing the inflow face.
2: If the triangle has two inflow sides, the residual is split over the two downstream nodes. The two subresiduals are formed by decomposing the convection speed as the sum of two components, each pointing along an inflow edge.

The scheme is monotonic and exact if the convection speed is aligned with any of the edges. Written as a general formula one obtains for the residual fraction sent to node i :

$$\phi_i^N = \frac{1}{2}k_i^{+}(w_i - w^{-}), \text{ with } w^{-} = \frac{\sum_j k_j^{-} w_j}{\sum_j k_j^{-}}. \tag{13}$$

The coefficients $k_j^{\pm}$ are defined by $k_j^{\pm} = \frac{1}{2}(\vec{\lambda}\cdot\vec{n}_j \pm |\vec{\lambda}\cdot\vec{n}_j|)$ where $\vec{n}_j$ are the scaled edge normals, figure 3. The state w^{-} can be interpreted as the value of w interpolated at the point where the convection speed enters the triangle.
In the present work we propose a generalization to arbitrary symmetrizable hyperbolic systems. Using the Jacobians based

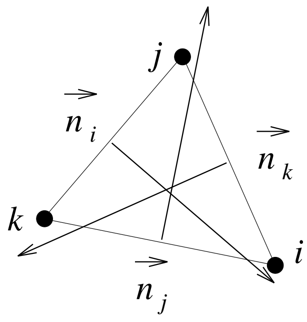

Figure 3. Normals for the N-scheme

on the edge-normals (figure 3), the distribution to node i is defined as:

$$\phi_i^N = \beta_i^N \phi^{\Omega} = \frac{1}{2}K_i^{+}(W_i - W^{-}), \tag{14}$$

where the state W^{-} is now defined as

$$W^{-} = \left(\sum_j K_j^{-}\right)^{-1} \sum_j K_j^{-} W_j. \tag{15}$$

It is easy to verify that if system (1) can be diagonalized, this system scheme reduces to the scalar N-scheme applied to each of the decoupled equations individually. Wellposedness of the scheme (existence of $\left(\sum_j K_j^{-}\right)^{-1}$) has been demonstrated by Abgrall, while positivity and moreover energy stability for symmetrizable linear systems was shown by Barth.

3.3 Comparison of first order results

Although the N-scheme is still a linear scheme, and therefore only first order accurate, it is much more accurate than the system FV-scheme on the median dual grid. This is illustrated by comparing the solutions for a subsonic NACA0012 airfoil at $M_\infty = .63$, $\alpha = 2°$. Both schemes are applied to the preconditioned equations (see below). The unstructured mesh shown in figure 4(a) has 2355 nodes of which 140 on the airfoil. The Mach distribution over the airfoil, figure 4(b), shows clearly the better capturing of the suction peak by the N-scheme. A grid converged solution has a suction peak close to $\mathrm{M} = 1$.

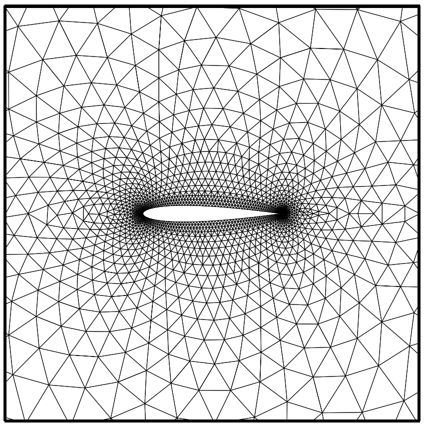

(a) Grid for the transonic NACA-0012, 2355 nodes

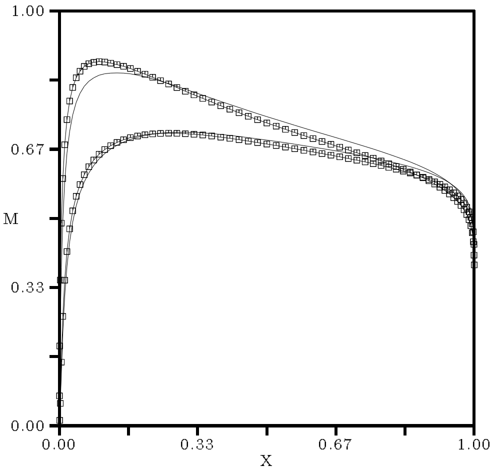

(b) Mach number distribution on the airfoil

Figure 4. Mesh and Mach number distribution on the airfoil for the HE splitting for the 1^{st} order system N-scheme (symbols indicating meshpoints) and system FV-scheme (straight line) for the subsonic NACA-0012 airfoil ($\mathrm{M}_\infty = 0.63, \alpha = 2^\circ$).

4 SIMILARITY TRANSFORMATIONS AND PRECONDITIONING

4.1 Invariance for similarity transformations

An important property of both the system FV- and the system N-scheme is that the residual sent to the nodes in conservative variables is independent of the choice of variables used for the actual distribution. Therefore characteristic decompositions based on similarity transformations, such as the pseudo-Mach angle model [6] or Deconinck-Hirsch decomposition [1] all lead to the same result. To show this, consider the set of (e.g. characteristic) variables $\partial \mathrm{V} = \frac{\partial \mathrm{V}}{\partial \mathrm{W}} \partial \mathrm{W}$. The hyperbolic system (1) transforms into

$$\frac{\partial \mathrm{V}}{\partial \mathrm{t}} + \mathrm{A_V} \frac{\partial \mathrm{V}}{\partial \mathrm{x}} + \mathrm{B_V} \frac{\partial \mathrm{V}}{\partial \mathrm{y}} = 0, \tag{16}$$

where

$$\mathrm{A_V} = \frac{\partial \mathrm{V}}{\partial \mathrm{W}} \mathrm{A_W} \frac{\partial \mathrm{W}}{\partial \mathrm{V}}, \quad \mathrm{B_V} = \frac{\partial \mathrm{V}}{\partial \mathrm{W}} \mathrm{B_W} \frac{\partial \mathrm{W}}{\partial \mathrm{V}}, \tag{17}$$

and so

$$\mathrm{K_i^{V+}} = \frac{\partial \mathrm{V}}{\partial \mathrm{W}} \mathrm{K_i^{W+}} \frac{\partial \mathrm{W}}{\partial \mathrm{V}}, \quad \mathrm{K_i^{V-}} = \frac{\partial \mathrm{V}}{\partial \mathrm{W}} \mathrm{K_i^{W-}} \frac{\partial \mathrm{W}}{\partial \mathrm{V}}. \tag{18}$$

Hence, the update for the N-scheme in conservative W variables when the distribution is calculated in characteristic variables V is given by

$$\begin{aligned} \phi_\mathrm{i}^\mathrm{N} &= \frac{\partial \mathrm{W}}{\partial \mathrm{V}} \frac{1}{2} \mathrm{K_i^{V+}} \left(\mathrm{V_i} - \mathrm{V^-} \right) \\ &= \frac{1}{2} \frac{\partial \mathrm{W}}{\partial \mathrm{V}} \mathrm{K_i^{V+}} \frac{\partial \mathrm{V}}{\partial \mathrm{W}} \frac{\partial \mathrm{W}}{\partial \mathrm{V}} \left(\mathrm{V_i} - \mathrm{V^-} \right) \\ &= \frac{1}{2} \mathrm{K_i^{W+}} \left(\mathrm{W_i} - \mathrm{W^-} \right), \end{aligned} \tag{19}$$

which is identical to (14) obtained by applying the system N-scheme directly to the variables W. A similar reasoning holds for the FV scheme.

4.2 Preconditioned equations

However, the results for steady flow can be improved if the schemes are applied to preconditioned pseudo-unsteady Euler equations. This preconditioning was originally developed by van Leer et al. [12] to speed up convergence. Roe [10] observed that these preconditioned equations lead to an optimally decoupled form of the steady Euler equations (hyperbolic-elliptic splitting) as discussed in the introduction. Consider the set of preconditioned equations in any convenient set of variables V, where P^{-1} is the preconditioning matrix :

$$\frac{\partial \mathrm{V}}{\partial \mathrm{t}} + \mathrm{P}^{-1} (\mathrm{A_V} \frac{\partial \mathrm{V}}{\partial \mathrm{x}} + \mathrm{B_V} \frac{\partial \mathrm{V}}{\partial \mathrm{y}}) = 0, \tag{20}$$

The eigenvalues of the Jacobian $\tilde{\mathrm{K}} = \mathrm{P}^{-1} (\mathrm{A_V n_x} + \mathrm{B_V n_y})$ have clearly changed and so will the distributed residual in conservative variables, which is now based on optimally decoupled Jacobians :

$$\phi_\mathrm{i}^\mathrm{N} = \frac{\partial \mathrm{W}}{\partial \mathrm{V}} \mathrm{P} \frac{1}{2} \tilde{\mathrm{K}}_\mathrm{i}^+ \left(\mathrm{V_i} - \mathrm{V^-} \right). \tag{21}$$

In particular, total enthalpy is now treated by a scalar convection scheme along the streamline which leads to improvements in the numerical results as will be discussed below.

5 NONLINEAR SECOND ORDER MATRIX DISTRIBUTION SCHEMES

For practical calculations the accuracy of the first order schemes described in section 3 is too low. An elegant way for constructing second order schemes from these first order schemes while keeping the positivity property is given by Sidilkover [11], see also [7]. For the *scalar* case, the distribution coefficients $\beta^{2\mathrm{nd}}$ of the second order limited scheme are simply obtained starting from the coefficients of the first order scheme by the following limiting procedure :

$$\beta_{\mathrm{i}}^{2\mathrm{nd}} = \frac{\max\left(0,\beta_{\mathrm{i}}^{1\mathrm{st}}\right)}{\sum_{\mathrm{j}} \max\left(0,\beta_{\mathrm{j}}^{1\mathrm{st}}\right)}, \tag{22}$$

or, in terms of distributed residuals to the nodes :

$$\phi_{\mathrm{i}}^{2\mathrm{nd}} = \frac{\max\left(0,\beta_{\mathrm{i}}^{1\mathrm{st}}\right)}{\sum_{\mathrm{j}} \max\left(0,\beta_{\mathrm{j}}^{1\mathrm{st}}\right)}\phi^{\Omega}. \tag{23}$$

It is easy to verify that the resulting scheme is linearity preserving ($\beta_{\mathrm{i}}^{2\mathrm{nd}}$ is bounded) and still positive ($\phi_{\mathrm{i}}^{2\mathrm{nd}} = \mathrm{C}\phi_{\mathrm{i}}^{1\mathrm{st}}$, where $\mathrm{C} \geq 0$), while preserving the compact Galerkin stencil of the original first order scheme.
The generalization to systems is however not trivial and many possibilities exist, while a systematic theory is still not available. To show these possibilities, we first present a limiting for the FV-scheme, based on Sidilkover's work [11].

5.1 Limited FV-scheme (LFV)

A compact limited FV-scheme (completely different from the standard MUSCL limited schemes) is obtained as follows : Define the three subresiduals ϕ_{12}, ϕ_{23} and ϕ_{31} in equation (11) by

$$\phi_{\mathrm{ij}} = \mathrm{K}_{\mathrm{ij}}\left(\mathrm{W}_{\mathrm{j}} - \mathrm{W}_{\mathrm{i}}\right), \tag{24}$$

and the matrices $\mathrm{I}_{\mathrm{ij}}^{+}$ and $\mathrm{I}_{\mathrm{ij}}^{-}$

$$\begin{aligned} \mathrm{I}_{\mathrm{ij}}^{+} &= \mathrm{K}_{\mathrm{ij}}^{-1}\mathrm{K}_{\mathrm{ij}}^{+} = \mathrm{R}_{\mathrm{ij}}\Lambda_{\mathrm{ij}}^{-1}\Lambda_{\mathrm{ij}}^{+}\mathrm{L}_{\mathrm{ij}} \\ \mathrm{I}_{\mathrm{ij}}^{-} &= \mathrm{K}_{\mathrm{ij}}^{-1}\mathrm{K}_{\mathrm{ij}}^{-} = \mathrm{R}_{\mathrm{ij}}\Lambda_{\mathrm{ij}}^{-1}\Lambda_{\mathrm{ij}}^{-}\mathrm{L}_{\mathrm{ij}}, \end{aligned} \tag{25}$$

such that $\mathrm{I}_{\mathrm{ij}}^{+} + \mathrm{I}_{\mathrm{ij}}^{-} = \mathrm{I}$, the unit matrix. With these definitions the distribution of the first order system FV-scheme, equation (12), can be written as

$$\phi_{\mathrm{i}}^{\mathrm{FV}} = \beta_{\mathrm{i}}^{\mathrm{FV}}\phi^{\Omega} = \mathrm{I}_{\mathrm{ij}}^{+}\phi_{\mathrm{ij}} + \mathrm{I}_{\mathrm{ki}}^{-}\phi_{\mathrm{ki}}, \tag{26}$$

where $(\mathrm{i,j,k})$ is again any circular permutation of $(1,2,3)$. The distribution to the nodes for the second order scheme is obtained by replacing ϕ_{ij}, ϕ_{ki} by their limited counterparts. These limited subresiduals are the result of applying the scalar limiting formula (23) componentwise to ϕ_{12}, ϕ_{23} and ϕ_{31}.

5.2 The limited N-scheme (LN or PSI)

A more systematic approach is followed aimed at a true matrix limiter. First, the scalar limiter expression (22) can be extended to systems as follows,

$$\beta_{\mathrm{i}}^{\mathrm{LN}} = \left(\sum_{\mathrm{j}} \beta_{\mathrm{j}}^{\mathrm{N}+}\right)^{-1} \beta_{\mathrm{i}}^{\mathrm{N}+}. \tag{27}$$

Here, $\beta_{\mathrm{i}}^{\mathrm{LN}}$ is the distribution matrix of the limited N-scheme to node i and $\beta_{\mathrm{i}}^{\mathrm{N}+}$ is the matrix based on the positive eigenvalues of the first order distribution matrix $\beta_{\mathrm{i}}^{\mathrm{N}}$, implicitly defined by

$$\beta_{\mathrm{i}}^{\mathrm{N}}\phi^{\Omega} = \frac{1}{2}\mathrm{K}_{\mathrm{i}}^{+}\left(\mathrm{W}_{\mathrm{i}} - \mathrm{W}^{-}\right). \tag{28}$$

However, since this equation fixes only 4 parameters (in 2D) some degrees of freedom in the definition of $\beta_{\mathrm{i}}^{\mathrm{N}}$ remain, except for a diagonal system. For the case of a diagonizable system the condition of invariance for similarity transformations is suffient to fix all parameters, giving

$$\beta_{\mathrm{i}}^{\mathrm{N}} = \mathrm{R}\mathrm{D}_{\mathrm{i}}\mathrm{L}, \tag{29}$$

where D_{i} is a diagonal matrix with k^{th} element $\mathrm{d}_{\mathrm{i}}^{\mathrm{k}}$ given by

$$\mathrm{d}_{\mathrm{i}}^{\mathrm{k}} = \frac{\mathrm{l}^{\mathrm{k}} \cdot \phi_{\mathrm{i}}^{\mathrm{N}}}{\mathrm{l}^{\mathrm{k}} \cdot \phi^{\Omega}}, \tag{30}$$

while L (with rows l^{k}) and R are the left and right eigenvector matrices of the K_{i}, which are independent of the normal.
A generalization for non-commuting systems used at present is

$$\beta_{\mathrm{i}}^{\mathrm{N}} = \mathrm{R}_{\mathrm{i}}\mathrm{D}_{\mathrm{i}}\mathrm{L}_{\mathrm{i}} + \frac{1}{3}\left(\mathrm{I} - \sum_{\mathrm{j}} \mathrm{R}_{\mathrm{j}}\mathrm{D}_{\mathrm{j}}\mathrm{L}_{\mathrm{j}}\right), \tag{31}$$

where R_{i} and L_{i} (with rows $\mathrm{l}_{\mathrm{i}}^{\mathrm{k}}$) contain the right respectively left eigenvectors of K_{i} and D_{i} is a diagonal matrix whose k^{th} element, $\mathrm{d}_{\mathrm{i}}^{\mathrm{k}}$, is given by

$$\mathrm{d}_{\mathrm{i}}^{\mathrm{k}} = \frac{\mathrm{l}_{\mathrm{i}}^{\mathrm{k}} \cdot \phi_{\mathrm{i}}^{\mathrm{N}}}{\mathrm{l}_{\mathrm{i}}^{\mathrm{k}} \cdot \phi^{\Omega}}. \tag{32}$$

The form (31), (which reduces to (29) for a diagonizable system) is not completely satisfactory in terms of robustness (see results section) and further improvements are under investigation.

5.3 Numerical results

To illustrate the possibilities of the new limited system distribution schemes, computations on two transonic flow test cases around a the NACA-0012 airfoil are shown, using the mesh allready presented in section 3.1, figure 6(a). Due to a lack of space only results with the limited N-scheme are given.

5.3.1 *Transonic NACA-0012,* $\mathrm{M}_{\infty} = 0.85$*,* $\alpha = 1°$

First, the convergence history (fig 5) is shown based on a Newton iterative solver [4]. The first order N-scheme shows full Newton convergence in 25 iterations. The second order computation is started from the first order solution, and the residual stagnates after about 6 orders of reduction (40 nonlinear iterations). Mach number isolines for the system limited N-scheme, applied to the preconditioned Euler equations are given in figure 6(a). The entropy distribution on the body, plotted in figure 6(b), compairs the limited N-scheme applied to the full Euler equations with the same scheme applied to the preconditioned equations (hyperbolic/elliptic splitting, HE). It is clear that the entropy production in the nose region is lower for the hyperbolic/elliptic splitting. Note that the entropy for both solutions remains perfectly monotonic in the shock. The most significant difference between both solutions however is found in the total enthalpy distribution : for the solution with hyperbolic-elliptic splitting total enthalpy remains perfectly constant, also in the shock profile and at the leading edge, as shown in figure 6(c).

5.3.2 Transonic NACA-0012, $\mathrm{M}_\infty = 0.80$, $\alpha = 1.25°$

Again the solution for the limited N-scheme with hyperbolic-elliptic splitting is shown. The weak shock on the pressure side is visible in the Mach number isolines, figure 7(a) and even clearer in the $\mathrm{C_p}$ distribution on the airfoil, figure 7(b). The entropy distribution on the airfoil is seen in figure 7(c) showing that shock capturing is perfectly monotonic also for entropy. However there is some production of entropy in the stagnation region, typical for a nonlinear monotonic scheme.

6 CONCLUSION

Positive, second order, monotonic matrix distribution schemes for hyperbolic systems have been presented, based on a compact stencil limiting. The numerical results confirm the monotonicity and show sharp capturing of the discontinuities. The schemes can be applied directly to the Euler equations, although application on the preconditioned Euler equations shows additional benefits for the steady flow Euler computations. Excellent convergence for a Newton iterative solver has been obtained.

ACKNOWLEDGEMENTS

Support by the European Space Agency (ESA) under contract No 9363/91/NL/FG/CCN2 and by the Commission of the European Union under Brite/EuRam contract AERO-CT-004/PL-2037 is gratefully acknowledged.

REFERENCES

[1] H. Deconinck, Ch. Hirsch, and J. Peuteman, 'Characteristic decomposition methods for the multidimensional Euler equations', *Lecture Notes in Physics, volume 264, Springer Verlag*, (1986).

[2] H. Deconinck, H. Paillère, R. Struijs, and P.L. Roe, 'A Multidimensional Generalization of Roe's Flux Difference Splitter for the Euler Equations', *Journal of Computers and Fluids, 22(2/3):215-222*, (1993).

[3] H. Deconinck, R. Struijs, G. Bourgois, and P.L. Roe, 'Compact Advection Schemes on Unstructured Grids', *VKI LS 1993-04, Computational Fluid Dynamics*, (1993).

[4] E. Issman, G. Degrez, and H. Deconinck, 'Implicit Upwind Residual-Distribution Euler and Navier-Stokes Solver on Unstructured Meshes', *AIAA J. Vol.35, no 3*, (1997).

[5] L.M. Mesaros and P.L. Roe, 'Multidimensional Fluctuation Splitting Schemes Based on Decomposition Methods', *AIAA Paper 95-1699, AIAA 12th CFD Conference, San Diego, CA*, (1995).

[6] H. Paillère, J.-C. Carette, and H. Deconinck, 'Multidimensional Upwind and SUPG methods for the Solution of the Compressible Flow Equations on Unstructured Grids', *VKI LS 1994-05, Computational Fluid Dynamics*, (1994).

[7] H. Paillère and H. Deconinck, 'Compact Multidimensional Upwind Convection Schemes on Unstructured Meshes', *Conf. on Num. Meth. for Euler and N-S equations, Montreal, Canada*, (1995).

[8] H. Paillère, H. Deconinck, and P.L. Roe, 'Conservative Upwind Residual-Distribution Schemes Based on the Steady Characteristics of the Euler Equations', *AIAA Paper 95-1700, AIAA 12th CFD Conference, San Diego, CA*, (1995).

[9] H. Paillère, E. van der Weide, and H. Deconinck, 'Multidimensional Upwind Methods for Inviscid and Viscous Compressible Flows', *VKI LS 1995-02, Computational Fluid Dynamics*, (1995).

[10] P.L. Roe, 'Multidimensional Upwinding: Motivation and Concepts', *VKI LS 1994-05, Computational Fluid Dynamics*, (1994).

[11] D. Sidilkover, 'Multidimensional Upwinding and Multigrid', *AIAA Paper 95-1759, AIAA 12th CFD Conference, San Diego, CA*, (1995).

[12] B. van Leer, W.T. Lee, and P. Roe, 'Characteristic Time-Stepping or Local Preconditioning of the Euler equations', *AIAA Paper 91-1552-CP, AIAA 10th CFD Conference*, (1991).

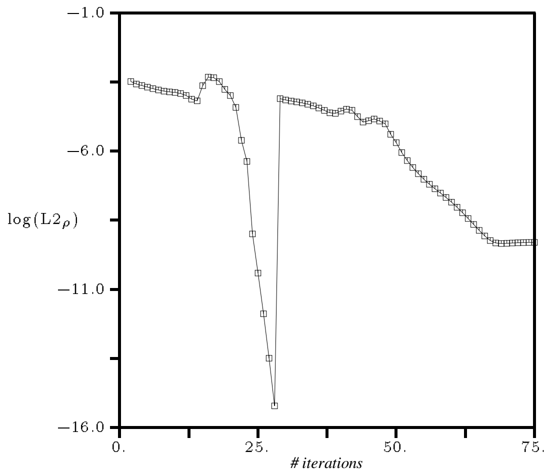

Figure 5. Convergence history for the HE splitting for the transonic NACA-0012 ($\mathrm{M}_\infty = 0.85$,$\alpha = 1°$) for the system N- (first part) and system limited N-scheme (second part) .

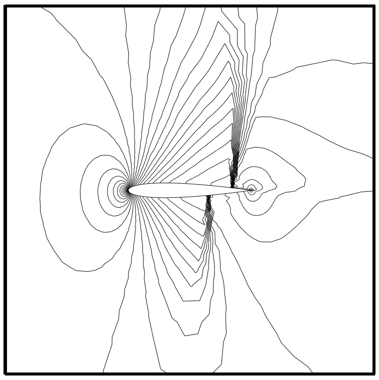

(a) Mach number isolines

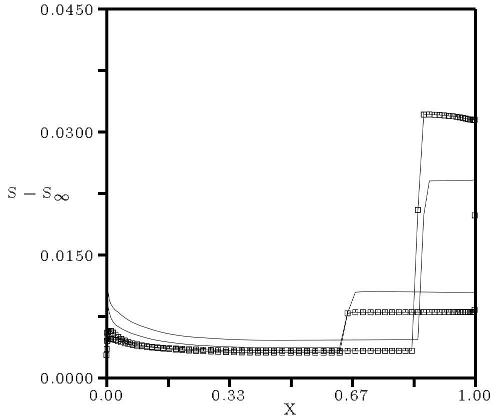

(b) Entropy distribution on the airfoil

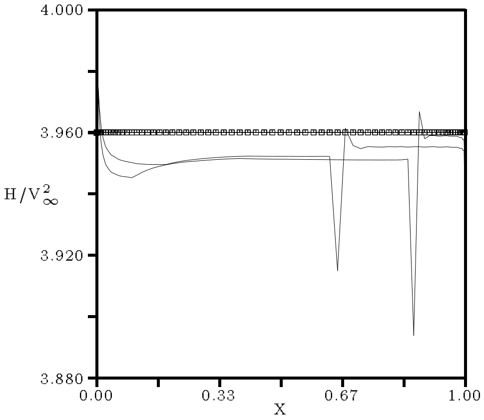

(c) Total Enthalpy distribution on the airfoil

Figure 6. Transonic NACA-0012 airfoil,$M_\infty = 0.85$,$\alpha = 1°$. System limited N-scheme. (a) : Mach number isolines for the HE splitting. (b),(c) : Entropy and Total enthalpy distribution on the airfoil for the preconditioned (symbols) and full (solid line) Euler equations.

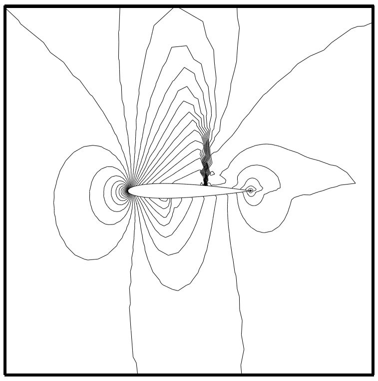

(a) Mach number isolines

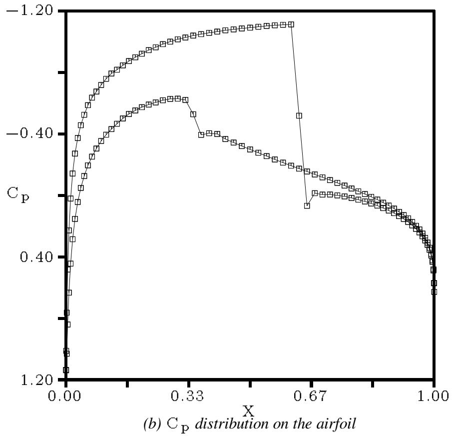

(b) C_p distribution on the airfoil

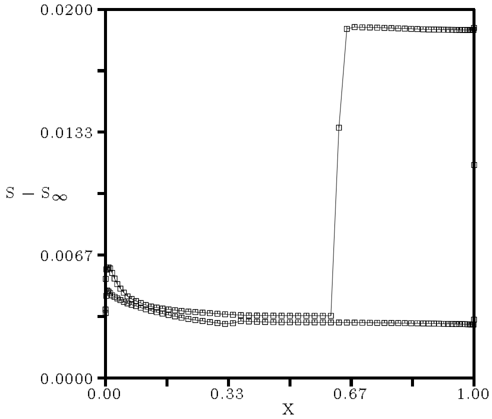

(c) Entropy distribution on the airfoil

Figure 7. Transonic NACA-0012 airfoil, $M_\infty = 0.80$,$\alpha = 1.25°$. System limited N-scheme. Mach number isolines, C_p distribution and Entropy distribution on the airfoil for the HE splitting.